Effect of a variety of carbon nanotubes on the iodine–iodide redox pair

Trevor J. Simmons [a,b,c,d,*], Noriko Maeda [b,c], Minoru Miyauchi [b,c,d,e], Jianjun Miao [b,c,e], Daniel P. Hashim [i], Pulickel M. Ajayan [i], Jonathan S. Dordick [a,b,c,e,f,g,h], Robert J. Linhardt [b,c,d]

[a] Center for Future Energy Systems, Rensselaer Polytechnic Institute, 110 8th Street, Troy, NY 12180, United States
[b] Rensselaer Nanotechnology Center, Rensselaer Polytechnic Institute, 110 8th Street, Troy, NY 12180, United States
[c] Center for Biotechnology & Interdisciplinary Studies, Rensselaer Polytechnic Institute, 110 8th Street, Troy, NY 12180, United States
[d] Chemistry & Chemical Biology, Rensselaer Polytechnic Institute, 110 8th Street, Troy, NY 12180, United States
[e] Chemical & Biological Engineering, Rensselaer Polytechnic Institute, 110 8th Street, Troy, NY 12180, United States
[f] Department of Biology, United States
[g] Department of Biomedical Engineering, Rensselaer Polytechnic Institute, 110 8th Street, Troy, NY 12180, United States
[h] Department of Material Sciences, Rensselaer Polytechnic Institute, 110 8th Street, Troy, NY 12180, United States
[i] Department of Mechanical Engineering & Materials Science, Rice University, 6100 Main Street, Houston, TX 77005, United States

ARTICLE INFO

ABSTRACT

The iodide (I^-)-triiodide (I_3^-) redox pair was used as a model system to evaluate the potential catalytic activity of various carbon nanotubes. Aqueous solutions of hydroiodic acid were irradiated with ultraviolet light in the presence of single wall, multi-wall, boron-doped and nitrogen-doped multi-wall carbon nanotubes. The nitrogen-doped multi-wall carbon nanotubes showed significant catalytic activity in the generation of hydrogen triiodide, while the other carbon nanotubes studied inhibited the generation of hydrogen triiodide. The photoconversion of hydroiodic acid to hydrogen triiodide, catalyzed by the nitrogen-doped multi-wall carbon nanotubes, was further accelerated by the presence of dissolved oxygen, offering an additional decomposition pathway for hydroiodic acid.

1. Introduction

Carbon nanotubes are a well-known allotrope of carbon consisting of cylindrical tubes of graphene (sp^2 bonded carbon sheets). These tubes can be either single-wall (SWCNT) or multi-wall (MWCNT), and can be doped with various elements such as nitrogen [1], boron [2], and phosphorus [3]. Nitrogen-doped multi-wall carbon nanotubes (CN_x-MWCNTs) are p-type doped carbon nanotubes, where the nitrogen atoms withdraw electron density from adjacent carbon atoms, creating partially positive charged centers on the MWCNT surface. These heterogeneous surface charges enable nitrogen-doped multi-wall carbon nanotubes (CN_x-MWCNTs) to exhibit significant catalytic properties, including catalyzing oxygen reduction reactions relevant to fuel cells and lithium air batteries. Dai and coworkers have suggested that the mechanism of this catalytic activity is based on the ability of both atoms of diatomic oxygen molecules to adsorb in parallel to the primary axis of CN_x-MWCNTs, rather than adsorb perpendicular to the CN_x-MWCNT primary axis as

with un-doped MWCNTs [4]. This is suggested to be due to the partially positive carbon atoms adjacent to the nitrogen doping sites.

The influence of CN_x-MWCNTs on a representative redox chemical reaction was investigated, and the CN_x-MWCNTs exhibited unique behavior compared to the other carbon nanotubes investigated. The aqueous Iodine–Iodide system is an important redox system, with applications ranging from dye-sensitized solar cells to antiseptics [5,6]. Since carbon nanotubes are incorporated into a wide variety of applications, ranging from dye-sensitized solar cells (DSSCs) [7], to antiseptic composites [6], to fuel cells [4], it is important to understand what impact carbon nanotubes doped with nitrogen and other elements may have in such systems.

In the current study the influence of SWCNTs, MWCNTs, CN_x-MWCNTs, and boron-doped multi-wall carbon nanotubes (CB_x-MWCNTs) on aqueous iodine–iodide redox chemistry was evaluated.

2. Experimental section

CN_x-MWCNTs were synthesized at Rice University using a floating catalyst aerosol-assisted chemical vapor deposition (AACVD) method, under atmospheric pressure conditions. Briefly, the chemical precursors used were a mixture of xylene (25 vol%) and acetonitrile (75 vol%) with ferrocene added (22 mg/mL) at a growth temperature of 850 °C. Argon/hydrogen (15% balance) gas was used to carry the nebulized precursor at a flow rate of 1.00 standard L/min and a precursor feed rate of 0.4 mL/min through a quartz tube furnace where the CN_x-MWCNT materials were deposited onto Si wafers and collected after synthesis. The total nitrogen content of the CN_x-MWCNTs was estimated at approximately 2.0% (+/−0.5%) based on X-ray photoelectron spectroscopy [8].

CB_x-MWCNTs were also synthesized at Rice University using AACVD as outlined above. Full details can be found elsewhere [2], but briefly, precursor solutions were prepared mixing toluene and ferrocene at a concentration of 25 mg/mL, and triethylborane at Fe:B ratio 5:1, followed by 30 min sonication. The major bonding state is B-substituted-C and BC_2O on the CB_x-MWCNT surface, and the boron content was estimated to be approximately 0.7% by X-ray photoelectron spectroscopy.

SWCNTs and MWCNTs were purchased from Swan Chemical, Inc. (Lyndhurst, NJ) as a wet cake material (Elicarb) composed of 90 wt.% water and 10 wt.% CNT, and were used as received.

The SWCNT and MWCNT material has less than 5 wt.% inorganic ash content and less than 3 wt.% iron content according to the certificate of analysis from the manufacturer. The SWCNT diameters were approximately 2 nm and 1 μm in length, and the MWCNT diameters were 12 nm and 10–100 μm in length. The CB_x-MWCNTs had diameters ranging from 40 to 150 nm and 5 to 100 microns in length, with a residual ash content of 5.1 wt.% after oxidation at 800 °C. The CN_x-MWCNTs had diameters ranging from 10 to 50 nm and 10 to 100 μm in length, with a residual ash content of 6.3 wt.% after oxidation at 800 °C.

Hydroiodic acid (HI) acid (57 wt.%) was purchased from Sigma–Aldrich (St. Louis, MO) and used as received.

Ultraviolet (UV) illumination was carried out with 96 W UV-A light source (Syngene GVM-30, Frederick, MD), maintained at a distance of 35 cm from illuminated samples.

Centrifugal separation of CNT solids from supernatant solutions was carried out in centrifuge 5804 (Eppendorf, Hauppauge, NY) operating at 5000 RPM for 3 min at 22 °C.

3. Results and discussion

Aqueous solutions of hydroiodic acid are converted to iodine when exposed to air for prolonged periods, as described in the reaction shown in Eq. (1) [9].

$$4HI + O_2 \rightarrow 2H^+ + 2I^- + I_2 + O_2^- \rightarrow 2H^+ + 2I_2 + 2H_2O_2^-$$
$$\rightarrow 2I_2 + 2H_2O$$
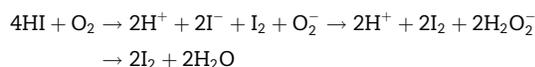
Eq. (1). Oxidation of hydroiodic acid to iodine via superoxide free radical intermediate.

Exposure of aqueous solutions of hydroiodic acid to light, particularly UV light, results in the reaction shown in Eq. (2) [10,11].

$$3H\,I + h\nu \rightarrow 2H^- + I_2 \rightarrow H_2 + I_2$$
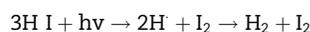
Eq. (2). Photoconverstion of hydroiodic acid to hydrogen and iodine via hydrogen free radical intermediate.

Triiodide is formed in equilibrium with iodine and iodide as shown as Eq. (3).

$$I_2 + I^- \rightleftharpoons I_3^-$$
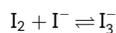
Eq. (3). Equilibrium of iodine and iodide with triiodide.

The two reactions described in Eqs. (1) and (2) proceed through free radical intermediates. Carbon nanotubes have
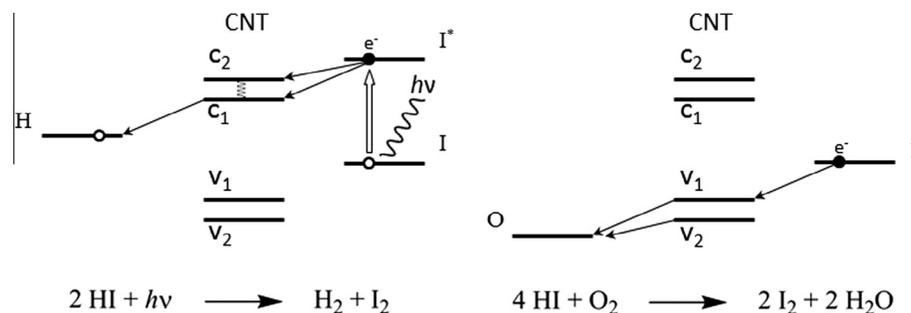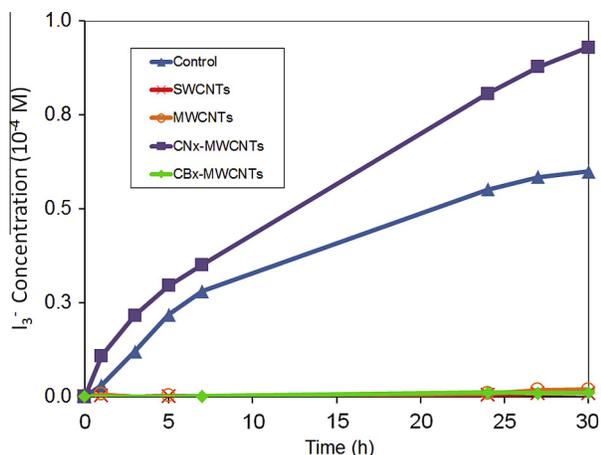

Fig. 1 – Schematic energy level diagrams for CN_x-MWCNTs in an aqueous solution of HI acid in the presence of UV light (left) and dissolved oxygen (right).

Fig. 2 – Hydroiodic acid solutions irradiated with a UV-A light source. The control sample was 20 mL neat 6 mM HI acid, and all other samples were 20 mL 6 mM HI acid with 10 mg CNTs added. CN$_x$-MWCNTs enhanced the photoconversion of HI to HI$_3$, forming nearly 60% more triiodide than the control sample. CB$_x$-MWCNTs and SWCNTs inhibited the conversion of HI to HI$_3$.

the potential to either promote or inhibit this pathway, which is largely dependent on their composition and presence of structural defects. Pristine SWCNTs and MWCNTs, along with CB$_x$-MWCNTs, are known to act as antioxidants [12]. SWCNTs and MWCNTs have been shown to exhibit free radical scavenging and halogen adsorption [12,13]. Doping of MWCNTs with boron (CB$_x$-MWCNTs) results in enhanced radical scavenging [12]. However, Hurt et al. have shown that structural defects present in SWCNTs and MWCNTs can have antioxidant deactivating properties [14]. This finding is supported by another report from Jafvert et al., which showed that carboxylic acid groups functionalized SWCNTs produced reactive oxygen free radicals in water when exposed to sunlight [15]. CN$_x$-MWCNTs have been reported to promote redox chemistry involving free radicals, such as the oxygen reduction reactions, which are particularly important in fuel cells

[4,16,17]. The reactions shown in Eqs. (1) and (2) are free radical reactions which have the potential to be catalyzed by CN$_x$-MWCNTs (Fig. 1).

The results of UV-A light exposure studies on various carbon nanotubes in 6 mM hydroiodic acid solution afforded results consistent with previous reports (Fig 2) [12,13].

A control sample of hydroiodic acid containing no carbon nanotubes showed moderate conversion of the HI to HI$_3$ after 30 h exposure to a UV-A light source. CN$_x$-MWCNTs substantially increased this photoconversion, while the SWCNTs and the CB$_x$-MWCNTs apparently inhibited this photoconversion. While the SWCNTs and CB$_x$-MWCNTs can scavenge the hydrogen and hydrogen peroxide free radicals produced under UV-A irradiation (Eq. 2) [18], CN$_x$-MWCNTs actually increase the rate of the oxidation of the HI to form hydrogen triiodide (Eq. 1).

A series of redox experiments were carried out at different temperatures to further examine the increased production of hydrogen triiodide in the presence of CN$_x$-MWCNTs. As the solution temperature increases, the equilibrium shown in Eq. (3) shifts to the left, with the concentration of I$_2$ nearly doubling as the temperature increases from 20 to 40 °C [19]. Hydroiodic acid (6 mM) exposed to UV-A light undergoes partial conversion to hydrogen triiodide at lower temperatures (Fig 3, left), but no conversion of HI to HI$_3$ was observed at 60 °C. Samples of hydroiodic acid in the presence of CN$_x$-MWCNTs at 60 °C, were partially converted to hydrogen triiodide in the dark and more so upon exposure to UV-A irradiation (Fig 3, right).
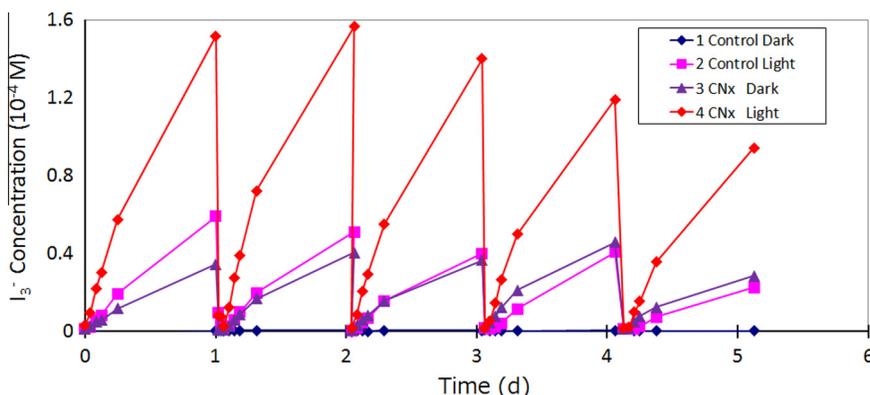
The conversion of hydroiodic acid to hydrogen triiodide in the presence of CN$_x$-MWCNTs in the dark (Fig 3, right, diamonds) follows the oxygen reduction reaction shown in Eq. (1). The hydroiodic acid irradiated with UV-A light in the presence of CN$_x$-MWCNTs undergoes both catalytic oxidation (Eq. 1) and photochemical oxidation (Eq. 2). CN$_x$-MWCNTs enable photochemical oxidation even at elevated temperature where this is typically inhibited. This strongly suggests that there the catalytic properties of CN$_x$-MWCNTs extends beyond the oxygen reduction reaction to the photochemical oxidation.
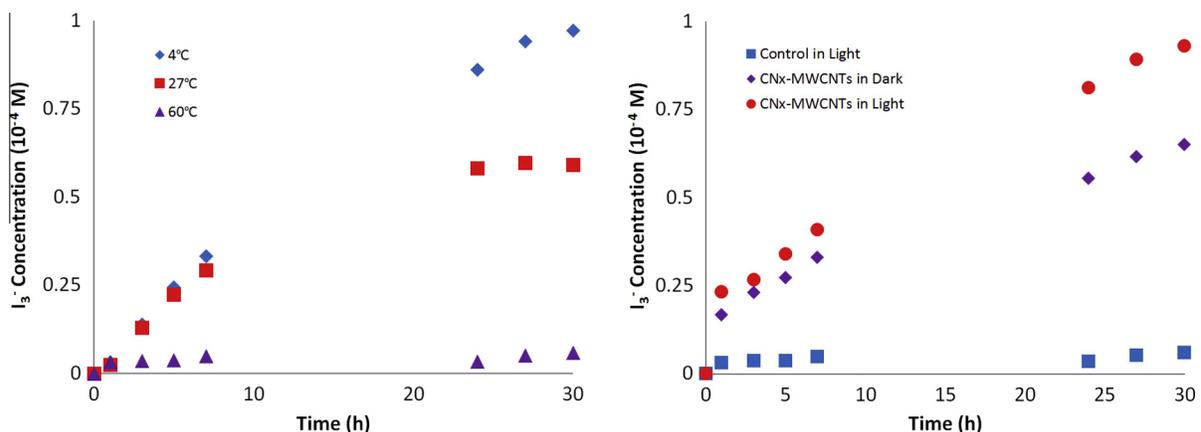
Fig. 3 – Hydroiodic acid solutions (6 mM) exposed to UV-A light at various temperatures (left) and at 60 °C (right) in the presence (UV-A and dark conditions) and absence (UV-A illuminated) of CN$_x$-MWCNTs. The control sample run at 60 °C (right) was neat 6 mM HI acid.
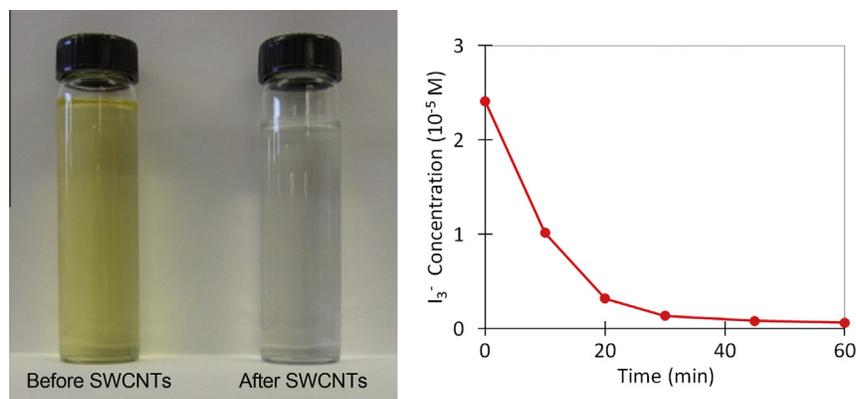
Fig. 4 – Aqueous solutions of 6 mM hydroiodic acid (left) after 24 h exposure to UV-A light, before (left) and after (right) exposure to SWCNTs. The presence of the triiodide ion is evident in the 'before' sample, and the yellow color is the result of two strong absorbance peaks at 288 nm and 350 nm [22]. Spectrophotometric results (right) showing that as SWCNTs are added to a solution of triiodide ($[I_3^-] = 2.4 \times 10^{-5}$ M, far left), nearly complete removal of triiodide occurs after 1 h. (For interpretation of the references to colour in this figure legend, the reader is referred to the web version of this article.)

Fig. 5 – Hydroiodic acid solutions (6 mM) under various conditions over 5 days. The combination of CN_x-MWCNTs and UV-A irradiation resulted in the greatest conversion of hydroiodic acid to hydrogen triiodide. The control sample was maintained in the dark and showed no appreciable conversion of hydroiodic acid to hydrogen triiodide. Solutions were 'reset' each day by a 1 h exposure to 1 mg SWCNTs to remove hydrogen triiodide.

The ability of the CN_x-MWCNTs to enhance the conversion of hydroiodic acid to hydrogen triiodide was further examined in a series of cycling experiments. Various hydroiodic acid samples were incubated in darkness or exposed to UV-A light, in the presence and absence of CN_x-MWCNTs. Previous studies have demonstrated that polyiodides such as I_2, I_3^-, and I_5^- intercalate into SWCNT bundles [20,21]. Therefore a cleanup procedure employing SWCNTs was developed based on this polyiodide intercalation to enable recycling of hydroiodic acid solutions that had been partially converted to hydrogen triiodide. This experiment consisted of adding 1 mg of SWCNTs to 20 mL of 6 mM hydroiodic acid that had been photochemically decomposed at room temperature for 24 h. The initial concentration of hydrogen triiodide was 2.4×10^{-5} M, and within 1 h of continued stirring at room temperature this concentration was reduced by more than 97%, to a concentration of 6×10^{-7} M (Fig 4). No surfactants were used to disperse the SWCNTs and therefore nearly all the SWCNTs were in the form of large bundles suitable for intercalation of polyiodides.

This effective removal of hydrogen triiodide from solution by the SWCNTs facilitated cycling evaluation. Hydroiodic acid solutions were exposed to CN_x-MWCNTs for 24 h both in the dark and with UV-A irradiation. Next the CN_x-MWCNTs were removed by centrifugation, the supernatant was exposed to SWCNTs for 1 h, after which the SWCNTs were removed by centrifugation. The next cycle was begun by the addition of fresh CN_x-MWCNTs for another 24 h exposure, enabling the effective cycling shown in Fig 5.

The results of the cycling experiments were in agreement with our initial studies. The total amount of hydrogen triiodide produced in the 24 h periods was reduced after the first cycle for the control in UV-A light and CN_x-MWCNTs in the dark, while the CN_x-MWCNTs in UV-A light reduced after the second cycle. The dark control remained constant over the entire study. This reduction over continued cycles was expected as the SWCNTs remove significant amounts of triiodide from the solutions.

4. Conclusions

The CNTs studied in this work have shown two distinct effects. The SWCNTs, MWCNTs, and CB_x-MWCNTs studied inhibited the photoconversion of aqueous solutions of hydroiodic acid to hydrogen triiodide. Based on this result, these materials would be best employed at the counter electrode of DSSCs where reduction of triiodide to iodide is desired. These materials should be employed with caution at the working electrode of DSSCs where triioide production is desirable. In contrast, the CN_x-MWCNTs studied promoted the photoconversion of the aqueous hydroiodic acid solutions to hydroiodic acid, and dramatically increased the rate of oxidation by dissolved oxygen. Based on these results, the recommendation would be to employ CN_x-MWCNTs at the working electrode of DSSCs, and to assure that oxygen has been excluded from the cell. SWCNT bundles removed polyiodides from solution by an intercalation process, consistent with previous reports [21]. This interaction between SWCNT bundles and polyiodides should be taken into consideration when employing SWCNTs in dye sensitized solar cells (DSSCs), as this behavior may affect cell efficiency. In most cases it would not be desirable for this intercalation to occur, and the SWCNTs should be thoroughly de-bundled prior to integration into a DSSC. Those using CN_x-MWCNTs [23], CB_x-graphene [24], and CB_x-MWCNTs in DSSCs that employ the iodide-triiodide redox pair should consider the results of this report.

Acknowledgments

REFERENCES

[1] Stephan O, Ajayan PM, Colliex C, Redlich P, Lambert JM, Bernier P, et al. Doping graphitic and carbon nanotube structures with boron and nitrogen. Energy Environ Sci 1994;266(5191):1683–5.

[2] Hashim DP, Narayanan NT, Romo-Herrera JM, Cullen DA, Hahm MG, Lezzi P, et al. Covalently bonded three-dimensional carbon nanotube solids via boron induced nanojunctions. Sci Rep 2012;2:363.

[3] Maciel IO, Campos-Delgado J, Cruz-Silva E, Pimenta MA, Sumpter BG, Meunier V, et al. Synthesis, electronic structure, and raman scattering of phosphorus-doped single-wall carbon nanotubes. Nano Lett 2009;9(6):2267–72.

[4] Gong KP, Du F, Xia ZH, Durstock M, Dai LM. Nitrogen-doped carbon nanotube arrays with high electrocatalytic activity for oxygen reduction. Energy Environ Sci 2009;323:760–4.

[5] Oregan B, Gratzel M. A low-cost, high-efficiency solar-cell based on dye-sensitized colloidal TiO2 films. Nature 1991;353(6346):737–40.

[6] Simmons TJ, Lee S-H, Park T-J, Hashim DP, Ajayan PM, Linhardt RJ. Antiseptic single wall carbon nanotube bandages. Carbon 2009;47:1561–4.

[7] Lee KS, Lee WJ, Park N-G, Kim SO, Park JH. Transferred vertically aligned N-doped carbon nanotube arrays: use in dye-sensitized solar cells as counter electrodes. Chem Commun 2011;47:4264–6.

[8] Simmons TJ, Hashim DP, Zhan X, Bravo-Sanchez M, Hahm MG, Lopez-Luna E, et al. Functionalization of nitrogen-doped carbon nanotubes with gallium to form Ga-CN_x-multi-wall carbon nanotube hybrid materials. Nanotechnology 2012;12:325601-1–9.

[9] Wiberg E, Wiberg N, Holleman AF. Inorganic chemistry. San Diego: Academic Press; 2001. pp. 371, 432–433.

[10] Rollefson GK, Booher JE. The absorption spectrum and photochemical decomposition of hydriodic acid. J Am Chem Soc 1931;53(5):1728–32.

[11] Takabayashi S, Nakamura R, Nakato Y. A nano-modified Si/TiO2 composite electrode for efficient solar water splitting. J Photochem Photobiol A 2004;166:107–13.

[12] Watts PCP, Fearon PK, Hsu WK, Billingham NC, Kroto HW, Walton DRM. Carbon nanotubes as polymer antioxidants. J Mater Chem 2003;13:491–5.

[13] Lucente-Schultz RM, Moore VC, Leonard AD, Price BK, Kosynkin DV, Lu M. Antioxidant single-walled carbon nanotubes. J Am Chem Soc 2009;131(11):3934–41.

[14] Liu X, Sen S, Liu J, Kulaots I, Geohegan D, Kane A, et al. Antioxidant deactivation on graphenic nanocarbon surfaces. Small 2011;7(19):2775–85.

[15] Chen C-Y, Jafvert CT. Photoreactivity of carboxylated single-walled carbon nanotubes in sunlight: reactive oxygen species production in water. Environ Sci Technol 2010;44:6674–9.

[16] Maldonado S, Stevenson KJ. Direct preparation of carbon nanofiber electrodes via pyrolysis of iron(II) phthalocyanine: electrocatalytic aspects for oxygen reduction. J Phys Chem B 2004;108:11375–83.

[17] Maldonado S, Stevenson KJ. Influence of nitrogen doping on oxygen reduction electrocatalysis at carbon nanofiber electrodes. J Phys Chem B 2005;109:4707–16.

[18] Lee HM, Odde S, Mhin BJ, Suh SB, Kim KS. Hydrogen detachment of the hexahydrated hydroiodic acid upon attaching an excess electron. Mol Phys 2007;105(19–22):2577–81.

[19] Gottardi W. Chapter 8: iodine and iodine compounds. In: Block SS, editor. Disinfection, sterilization, and preservation. Philadelphia: Lea & Febiger; 1991. p. 152–65.

[20] Grigorian L, Williams KA, Fang S, Sumanasekera GU, Loper AL, Dickey E, et al. Reversible intercalation of charged iodine chains into carbon nanotube ropes. Phys Rev Lett 1998;80(25):5560–3.

[21] Zhao Y, Wei J, Vajtai R, Ajayan PM, Barrera EV. Iodine doped carbon nanotube cables exceeding specific electrical conductivity of metals. Sci Rep 2011;1:83.

[22] Wei YJ, Liu CG, Mo LP. Ultraviolet absorption spectra of iodine, iodide ion and triiodide ion. Spectrosc Spectral Anal 2005;25(1):86–8.

[23] Lee KS, Lee WJ, Park NG, Kimand SO, Park JH. Transferred vertically aligned N-doped carbon nanotube arrays: use in dye-sensitized solar cells as counter electrodes. Chem Commun 2011;47:4264–6.

[24] Lin T, Huang F, Liang J, Wang Y. A facile preparation route for boron-doped graphene, and its CdTe solar cell application. Energy Environ Sci 2011;4:862–5.